ACS APPLIED MATERIALS & INTERFACES

UNIVERSITY OF GOTHENBURG
GOTHENBURG UNIVERSITY LIBRARY

Subscriber access provided by Gothenburg University Library

Energy, Environmental, and Catalysis Applications

# Effect of interfacial water structure on the Hydrogen evolution Reaction on Pt(111) modified with different Nickel Hydroxide coverages in alkaline media.

Francisco J Sarabia, Paula Sebastian-Pascual, Marc Koper, Victor Climent, and Juan M. Feliu

*ACS Appl. Mater. Interfaces*, **Just Accepted Manuscript** • DOI: 10.1021/acsami.8b15003 • Publication Date (Web): 12 Dec 2018

**Downloaded from http://pubs.acs.org on December 13, 2018**

## Just Accepted

"Just Accepted" manuscripts have been peer-reviewed and accepted for publication. They are posted online prior to technical editing, formatting for publication and author proofing. The American Chemical Society provides "Just Accepted" as a service to the research community to expedite the dissemination of scientific material as soon as possible after acceptance. "Just Accepted" manuscripts appear in full in PDF format accompanied by an HTML abstract. "Just Accepted" manuscripts have been fully peer reviewed, but should not be considered the official version of record. They are citable by the Digital Object Identifier (DOI®). "Just Accepted" is an optional service offered to authors. Therefore, the "Just Accepted" Web site may not include all articles that will be published in the journal. After a manuscript is technically edited and formatted, it will be removed from the "Just Accepted" Web site and published as an ASAP article. Note that technical editing may introduce minor changes to the manuscript text and/or graphics which could affect content, and all legal disclaimers and ethical guidelines that apply to the journal pertain. ACS cannot be held responsible for errors or consequences arising from the use of information contained in these "Just Accepted" manuscripts.

ACS Publications

is published by the American Chemical Society. 1155 Sixteenth Street N.W., Washington, DC 20036

Published by American Chemical Society. Copyright © American Chemical Society. However, no copyright claim is made to original U.S. Government works, or works produced by employees of any Commonwealth realm Crown government in the course of their duties.

# Effect of interfacial water structure on the Hydrogen evolution Reaction on Pt(111) modified with different Nickel Hydroxide coverages in alkaline media.

Francisco J. Sarabia, Paula Sebastián-Pascual, Marc T.M. Koper,[1)] Victor Climent*, Juan M. Feliu*

Instituto Universitario de Electroquímica, Universidad de Alicante, Carretera San Vicente del Raspeig s/n, E-03690, San Vicente del Raspeig, Alicante, Spain

[1)]Leiden Institute of Chemistry, Leiden University, PO Box 9502, 2300 RA, Leiden, The Netherlands

Corresponding authors: victor.climent@ua.es juan.feliu@ua.es

**Abstract**

The hydrogen evolution reaction (HER) constitutes one of the most important reactions in electrochemistry due to the value of hydrogen as a vector for energy storage and transport. Therefore, understanding the mechanism of this reaction in relation to its pH-dependence is of crucial importance. While the HER on Pt(111) works efficiently in acid media, in alkaline media the reaction is impeded and considerably larger applied overpotentials are necessary. The presence of $Ni(OH)_2$ adsorbed on Pt(111) has been demonstrated to highly improve the rate of hydrogen evolution, decreasing the overpotential of this reaction in comparison to acid media. The way how low coverages of $Ni(OH)_2$ on the Pt surface improves HER is still under discussion. In this work, we have prepared different $Ni(OH)_2$ coverages on Pt(111) to check how $Ni(OH)_2$ deposited on Pt(111) influences the HER rate. To this end, the $Ni(OH)_2$-Pt(111)| 0.1M NaOH interface was characterized with cyclic voltammetry, CO displacement technique and FTIRRAS. Based on the proposal made by Ledezma-Yanez et. al. [Nature Energy 2017, 2, 17031] to explain the HER in alkaline media, we also studied the effect of the different $Ni(OH)_2$ coverages on the electric field using the laser induced temperature jump technique. This technique revealed that introduction of nickel adlayers on the surface decreases the ordering of the water network at the interphase, a fact that has relevant implications for the HER mechanism.

Keywords: hydrogen evolution reaction; platinum single crystal; potential of zero charge; potential of maximum entropy; nickel adlayers; interfacial water reorganization

## 1) Introduction

There is great interest nowadays in the so-called hydrogen economy as response to the necessity of improving the quality of the environment.[1] Although methods like photo-electrolysis or photocatalytic water splitting are the subject of intense development, large-scale energy storage through hydrogen production still depends on water electrolysis.[2] In this regard, better alkaline electrolyzers require an understanding of why there is an overpotential for the hydrogen evolution reaction (HER) in alkaline media as compared to acid media. The elucidation of the mechanism of this reaction at the molecular level and its dependence on solution pH are crucial starting points for the synthesis and development of economic materials that would allow reaching an efficient electrocatalysis.

It is known that platinum is the best catalyst for the HER. The mechanism for HER in alkaline media consists of a combination of three steps. First, the Volmer step involves water dissociation and formation of a reactive intermediate ($H_2O + M + e^- \leftrightarrow M\text{-}H_{ad} + OH^-$). This step can be followed by: one Tafel step where two $H_{ad}$ are recombined ($2M\text{-}H_{ad} \leftrightarrow 2M + H_2$) or one Heyrovsky step, with a second electronic transfer ($M\text{-}H_{ad} + H_2O + e^- \leftrightarrow M + H_2 + OH^-$).[3] It has been reported that $Ni(OH)_2$ adsorbed on Pt(111) improves the kinetics of HER in alkaline media. Subbaraman et al. have attributed this catalytic enhancement to the oxophilicity of nickel favoring water dissociation in the Volmer step by stabilizing the resulting $OH^-$ anion through a concerted interaction of water molecules at the $Ni(OH)_2$-Pt boundaries.[4] In this model, the sole parameter considered for the pH-dependence of the HER is the OH-binding energy to the $Ni(OH)_2$.[5]

In contrast to the model by Markovic et al., our groups in Alicante and Leiden have suggested that the addition of small amounts of $Ni(OH)_2$ to Pt(111) in alkaline media causes a decrease of the electric field due to a negative shift of the potential of zero free charge (pzfc)/ potential of maximum entropy (pme) toward the hydrogen region which results in a decrease in the energy of reorganization of the interfacial water. This allows an easier transport of $OH^-$ through the double layer.[6] This new model for HER is based on the idea that, in acid media, the pzfc/pme of Pt(111) is closer to the hydrogen region (as compared with the alkaline media) resulting in a less ordered interfacial water network that allows a more facile proton transfer through the double layer.

In this work, we present further evidence for the shift of the potential of zero total charge (pztc) and pzfc/pme toward less positive potentials for different $Ni(OH)_2$ coverages on Pt(111) using both the CO displacement technique and the laser-induced temperature-jump technique.[7] In addition, the shift is linked to the effect that nickel modification of the surface has on the HER rate.

## 2) Experimental

### *2.1) Chemicals*

0.1 M NaOH solutions were prepared using sodium hydroxide monohydrated (Merck Suprapur). The solution with pH 4.5, employed for the nickel deposition in the flow cell, was prepared using sodium fluoride (Sigma-Aldrich for analysis), perchloric acid (Merck suprapur) and nickel sulfate (Sigma-Aldrich 99.99%). All solutions were prepared using ultrapure water from Elga Purelab Ultra Analytic system (Resistivity 18.2 MΩ cm). Argon, hydrogen and CO (N50, Air liquid) were used for deaerating the solution, to cool down the electrode after the flame annealing and for the CO displacement experiments, respectively. Solutions were deaerated by bubbling Ar for at least 15 min and, during the experiments, an Ar blanket was maintained above the solution to prevent the entrance of $O_2$ into the cell. The pH of the solutions was measured using a pH-basic-20 pH-meter from Crison coupled with a pH-probe pH 50 12 HACH model.

### *2.2) Nickel hydroxide deposition*

$Ni(OH)_2$ deposition at the different coverages, except at the highest value, were carried out at open circuit potential by holding the Pt(111) electrode in a diluted aqueous solution of nickel sulphate during 10 s. Different nickel sulfate concentrated solutions, between $10^{-5}$ M and $10^{-2}$ M, were employed to achieve each $Ni(OH)_2$ coverage. Prior to modification, the electrode was flame annealed in a propane-oxygen flame and cooled down in a hydrogen/argon (1:3) atmosphere. The highest nickel hydroxide coverage was obtained using a flow cell that allowed keeping the electrode under potential control while the solution was replaced. For this experiment, the electrode potential was held at -0.37 V vs Ag/AgCl/KCl saturated reference electrode in a solution containing 10 mM $NiSO_4$ plus 40 mM of $NaF/HClO_4$ (at pH 4.5) buffer solution, for sufficient time to ensure whole surface nickel coverage (~5 min). This method is the same used previously to achieve the

maximum nickel coverage for a 2D deposit;[7] in this case, coverage calculations were achieved from a combination of voltammetric stripping charges and results of the CO charge displacement technique. We have previously shown that CO protects the nickel adlayer during solution exchange.[7] For that reason, prior to replacing the solution with nickel free electrolyte, CO was bubbled until the entire surface was blocked and the registered current dropped to zero. Then, the solution was replaced by freshly prepared 40 mM $NaF/HClO_4$, without nickel, before adding the freshly prepared 0.1 M NaOH solution, under CO bubbling. This sequence of steps was followed to avoid the precipitation of nickel hydroxide in the bulk solution. Before introducing the NaOH solution, the electrode potential was changed to -0.85 V vs Ag/AgCl/KCl saturated in order to avoid the oxidation of $Ni(OH)_2$-Pt(111) after the pH change from 4.5 to 13. Finally, the 0.1M NaOH solution was bubbled with Ar during 15 minutes to fully remove all traces of CO, and the adsorbed CO on the platinum surface was stripped. This methodology allows increasing the nickel coverage in comparison to the deposit prepared at open circuit potential.

### *2.3) Electrochemical experiments*

The experiments were performed at room temperature in a classical three electrode cell configuration using a Luggin capillary to separate the reference electrode from the main working solution. A coiled platinum wire was used as counter electrode. A Ag/AgCl/KCl saturated electrode was used as reference for FTIRRAS and high nickel hydroxide coverage experiments. A Pd-$H_2$ electrode was used as reference for the laser temperature jump technique, and a reversible hydrogen electrode (RHE) was used as reference for the rest of electrochemical experiments. The Luggin capillary was filled with the same solution as that of the main compartment of the cell. The working electrode was contacted with the solution in the hanging meniscus configuration. Potential control was attained with a potentiostat (eDAQ EA161) connected with a signal generator (PAR 173) and digital recorder (eDAQ, ED401).

### *2.4) CO displacement technique*

CO displacement experiments were performed by following the same methodology as previously reported.[8] The experiments consist of the following steps: I) After recording the voltammogram, potential cycling was stopped at 0.1 V. II) A flow of CO was introduced into the electrochemical cell while the transient current, produced in response to the introduction of this gas, was recorded. It is very important to avoid the entrance of $O_2$ into the experimental system by flushing permanently either Ar or CO. III) When current decays to zero, indicating saturation of the surface, the CO flow was stopped, and Ar was bubbled (during 15 min) into the solution to remove the excess CO dissolved in solution. IV) Next, the surface blockage was checked in the low potential range and finally, the CO adsorbed on the surface was stripped for recovery of the initial surface profile.

### *2.5) FTIRRAS*

In situ external reflection infrared experiments were carried out with a Nicolet 8700 (Thermo Scientific) spectrometer equipped with an MCT-A detector using p-polarized light and with a spectral resolution of 8 $cm^{-1}$. The glass spectroelectrochemical cell was equipped with a prismatic $CaF_2$ window beveled at 60°. A Ag/AgCl/KCl saturated electrode was used as reference in this case, but all potentials have been converted to the RHE scale. The Pt(111) working electrode used in these experiments was ca. 4.5 mm in diameter and was prepared and treated before experiments in a similar way as the smaller samples used in the voltammetric experiments. The spectra are plotted in absorbance units ($-\log(R/R_0)$) by referring the single beam reflectance spectrum collected at the sample potential (R) to the one collected at the reference potential ($R_0$). The reference potential was selected as 0.72 V for the study of the CO bands and 0.1 V for the study of carbonate bands. The methodology of this experiment consists of the following steps: I) The working electrode was introduced at 0.1 V in the solution, and CO was bubbled for 5 min to saturate the surface. II) Then, argon was bubbled to remove the CO from the solution and the electrode was pressed against the $CaF_2$ window, holding at all times the electrode potential at the initial value. III) Then, after recording the initial spectrum, the potential was sequentially stepped to increasing values and spectra were recorded at each potential until all CO was oxidized. 200 interferograms were collected at each potential.

### *2.6) Laser induced temperature jump technique*

The procedure for recording the laser induced transients was described in detail elsewhere.[9, 10] Before recording the laser transient, several voltammetric cycles were recorded to ensure the cleanliness and stability of the system. A second auxiliary electrode is used as an internal reference to measure the potential transient. At the beginning, both working and the second auxiliary electrode are polarized at the same potential and 200 μs before firing the laser both electrodes are disconnected from the potentiostat. Each experiment is repeated with a frequency of 10Hz to ensure that the temperature relaxes to the initial value between measurements. Either 128 or 256 potential transients are recorded and averaged using a Tektronix Model TDS 3054B oscilloscope.

The duration of the pulse is 5ns and the laser used is a 532 nm frequency (double harmonic) Nd-YAG (Brilliant B from Quantel). A standard arrangement of lenses is used to reduce the diameter of the laser beam from 6 mm to 4 mm. The energy density of the laser beam is reduced to less than 8 mJ/cm$^2$ by combining the effect of an attenuator from Newport Corporation (Model M-935-10) and the regulation of the Q-switch time. The laser energy was measured with a piroelectric sensor head (Model M-935-10).

## 3) Results and discussion

### *3.1) Voltammetric characterization of HER in modified Pt(111) by Ni(OH)$_2$*

The cyclic voltammetries of the Pt(111) surface with different nickel coverages, $\theta_{Ni(OH)2}$, from 0 to 0.37, in 0.1 M NaOH are shown in Figure 1A. Nickel coverage is calculated from the remaining voltammetric hydrogen charge as described in section 3.3. As the nickel coverage increases, the corresponding peak related to OH adsorption on the bare Pt(111) surface, centered at 0.77 V, decreases while a new anodic peak emerges at 0.7 V. This new peak increases in intensity as the nickel coverage grows. In the negative-going scan the corresponding cathodic peak appears centered at 0.55 V. The peak separation ($\Delta E_p$) is higher than 150 mV (at a sweep rate of 50 mV/s) evidencing that the redox process involved under these peaks is kinetically slow. The origin of the peak at 0.7 V is not clearly understood yet. Previous works reported that the peaks appearing around 0.7

V and 0.55 V were associated to the enhanced oxidative adsorption and the irreversible reductive desorption of OH ions respectively, on Pt zones nearby to nickel clusters.[2, 4] This shift in the hydroxide adsorption/desorption was related to the higher oxophilicity of the nickel species adsorbed on the electrode. According to these works, Ni adsorbed on the Pt(111) surface is in the +2 state, remaining in the $Ni(OH)_2$ form in the whole potential window studied in this work. XAS measurements revealed only a small increase in the nickel valence state up to 2.3 at the onset of the oxygen reduction reaction.[2] Subbaraman et.al. claimed that the phase of the nickel hydroxide species resembles that of $\beta$-$Ni(OH)_2$, and that it is stable at potentials below 1.5 V. $Ni(OH)_2$ is expected to oxidize to NiOOH at potentials higher than 1.5V.[2] However, if OH adsorption only takes place on the Pt-Ni adjacent sites, charge of the peak would scale with the perimeter of the islands. The linear relationship demonstrated below seems to indicate that this is not the case. Another possibility is that the irreversible redox process involves OH adsorption on nickel. This would imply a formal change in the nickel oxidation state (from +2 to +3) that seems to contradict the result of the XAS measurements. However, we need to consider that the formal oxidation state does not necessarily need to be equal to the true electronic state of Ni. In this case, the Ni-hydr(oxy)oxide species would be formed at potentials lower than expected, due to the effects of the platinum substrate on the electronic structure of the adlayer.[11] Finally, the voltammetric profiles show a corresponding decrease in the charge involved in the hydrogen UPD region (0.06-0.4 V vs RHE), when $Ni(OH)_2$ coverage increases.

Figure 1B shows the HER at different $Ni(OH)_2$ coverages. Despite the blockage of Pt sites available for hydrogen adsorption, the HER rate is actually enhanced with increasing $Ni(OH)_2$ coverage (figure 1B). At -0.088 V, the HER activity is enhanced by a factor of 9 to 43 relative to the bare Pt(111) (in terms of current density) for $Ni(OH)_2$ coverages of 0.07 and 0.37, respectively.

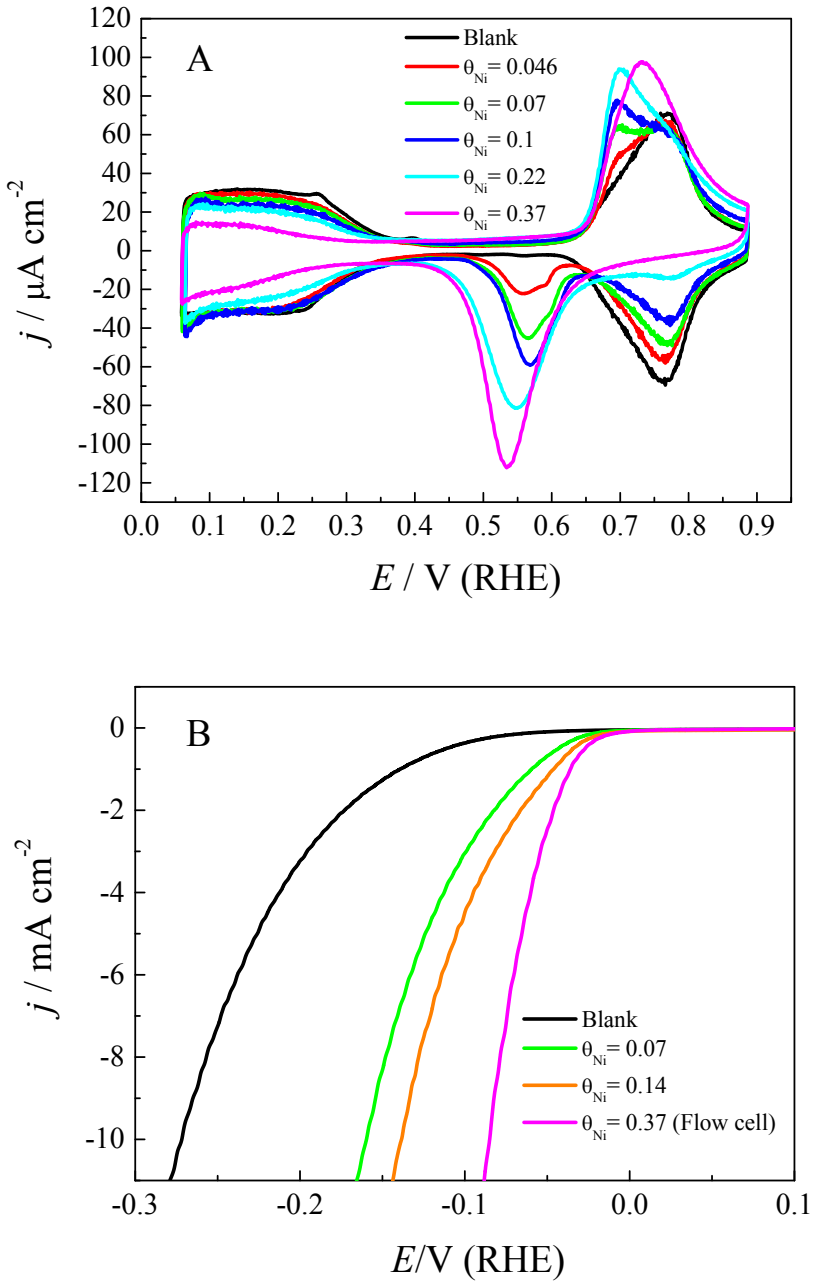


**Figure 1**. A) Cyclic voltammograms of the Pt(111) surface modified with different $Ni(OH)_2$ coverages and B) the same showing the hydrogen evolution reaction. The ohmic resistance was corrected for the HER. Scan rate 50mV/s. 0.1 M NaOH.

***3.2) CO oxidation on Ni(OH)2-Pt(111) spectroscopic analysis by FTIRR***

To obtain more evidence about how $Ni(OH)_2$ influences the charge redistribution at the Pt(111)/electrolyte interface, measurements with the CO displacement technique were performed. Before describing the CO displacement results, it is convenient to discuss first the process of CO oxidation on $Ni(OH)_2$-Pt(111), as studied with stripping voltammetry and FTIR spectroscopy. CO stripping is the last step in the CO displacement experiment and it is a typical probe reaction in surface electrochemistry. Fig. 2 shows the oxidation of the CO adsorbed on Pt(111) with different Ni(II) coverages. When the nickel coverage increases, the peak centered at 0.75 V vs RHE shifts to 0.7 V. At the same time, the pre-wave, observed around 0.65 V vs RHE on bare Pt(111), also shifts towards less positive potentials while its charge density increases. By increasing $Ni(OH)_2$ coverage, most of the CO oxidation takes place around 0.48V, evidencing a high catalytic activity in CO oxidation due to the $Ni(OH)_2$ adsorbed on the electrode surface.

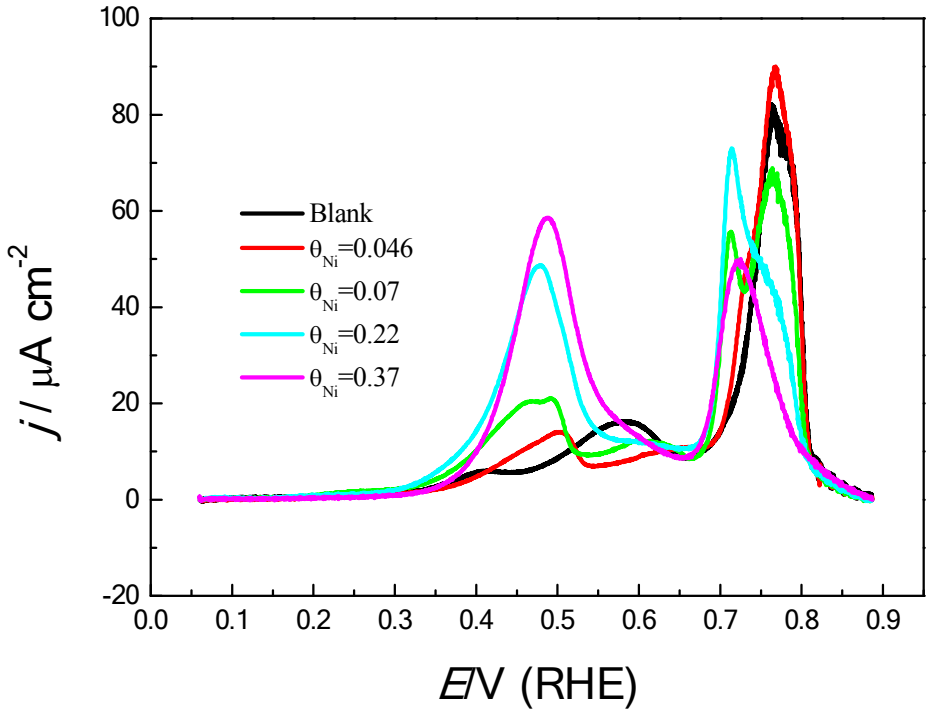


**Figure 2.** CO stripping on the $Ni(OH)_2$-Pt(111) modified surfaces with different Ni coverages ($\theta_{Ni}$ ) as indicated in the figure. Scan rate, 20mV/s. 0.1 M NaOH

Figure 3A-F contains FTIR spectra of bare and modified Pt(111) substrates. The spectra showing the bands for adsorbed CO on the surface were obtained by taking as reference

the spectrum recorded after CO oxidation (Fig 3A, 3C and 3E). On the other hand, absolute carbonate bands (1400 $cm^{-1}$) were more conveniently obtained by referencing the spectra to the spectrum recorded at 0.1 V (Fig. 3B, 3D and 3F). On the Pt(111) surface without nickel, two main CO bands were observed, at 2025 and 1800 $cm^{-1}$ that can be ascribed to on top and bridge CO, respectively (Fig. 3A) [12]. When Pt(111) is highly covered with nickel (Fig. 3E), the band corresponding to on top CO decreases strongly and the band corresponding to bridge CO disappears while another band appears at 1865 $cm^{-1}$. In accordance with these observations, we ascribe the band at 1865 $cm^{-1}$ to the CO adsorbed on metallic nickel[13-15] while the remaining small band at 2025 $cm^{-1}$ should correspond to CO adsorbed on the free Pt(111) sites not covered by $Ni(OH)_2$. As can be seen in figures 3A and 3E, the band centers associated to CO adsorbed on Pt or Ni sites undergo a slight Stark shift with the applied potential. Comparing the frequency of the band corresponding to CO adsorbed on metallic nickel in alkaline and acid media (pH=4.5),[7] we observe that the band center appears at markedly lower wavenumbers in the first one (1865 and 1900 $cm^{-1}$ for each media respectively). This displacement in the wavenumber is due to the change in the absolute potential versus the SHE, which is more negative in alkaline than in acid media. Plotting the wavenumber versus the potential (SHE) for both media, results in a straight line with average slope of 60 $cm^{-1}$ $V^{-1}$, demonstrating that both bands corresponds to the same vibration (figure S1). To obtain more insight, results for adsorbed CO on Pt(111)-$Ni(OH)_2$ at an intermediate coverage ($\theta_{Ni}$=0.20) are also shown in figure 3C. In this case, a band appearing at 1850 $cm^{-1}$ can be observed, which shows a small shoulder (marked with a black arrow in the figure). This shape is the result of the overlap of the corresponding bands associated to the CO adsorbed on Ni and Pt(111), with the shoulder being ascribed to the latter. As the potential is increased, the main band disappears and the shoulder emerges as a new band. This suggests a preferential oxidation of the CO adsorbed on nickel, in accordance with the voltammetric results of figure 2. Figure S2 plots the frequency of the bands indicated above as a function of potential. While at low potential the band around 1850 is clearly blueshifted in comparison with the corresponding blank experiment without Ni, above 0.42 V, i.e., after oxidation of CO on Ni, the frequency of the band recorded with and without Ni coincide reasonably well. All these results together give sufficient confidence in the assignment of the band at 1850 $cm^{-1}$ to the vibration of CO adsorbed on Ni. In this way, FTIR data provides unambiguous evidence of CO adsorption on $Ni(OH)_2$-Pt(111) surface.

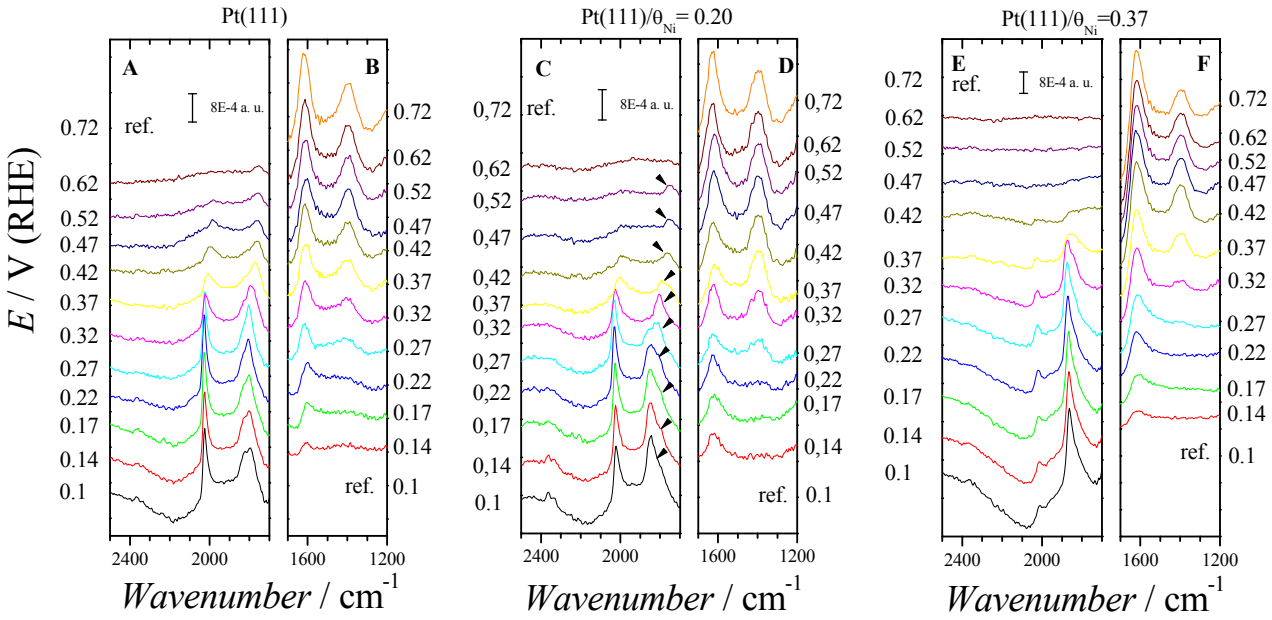


**Figure 3.** FTIR spectra of the CO adsorbed on the Pt(111) surface, A-B) without $Ni(OH)_2$, C-D) with $Ni(OH)_2$ $\theta_{Ni}$=0.20 and E-F) with $Ni(OH)_2$ $\theta_{Ni}$=0.37. The reference potential in each case is indicated in the figures. 200 interferograms were collected at each potential. Arrows in C mark the position of the band assigned to bridge CO on platinum sites (see text for details).

### *3.3) CO displacement measurements and coulometric analysis.*

After demonstrating that CO can adsorb on both Pt and Ni and assuming that fully blocks the $Ni(OH)_2$-Pt(111) surface forming Ni-CO/Pt-CO, several CO charge displacement measurements were analyzed to investigate how different amounts of $Ni(OH)_2$ modify the pztc of Pt(111).

Fig 4 shows the transient currents obtained during the CO displacement for Pt(111) electrode with and without $Ni(OH)_2$ adsorbed on the surface at pH 13. The holding potential was 0.1 V in all cases. For bare Pt(111), a positive current is observed during CO adsorption due to the displacement of hydrogen. The average integrated charge

involved in the CO displacement amounts to 126 μC/cm$^2$ at 0.1 V vs RHE, in accordance with previous reports.[16] When nickel coverage increases, two different contributions are observed during the CO displacement. Similar trends were already observed for nickel adlayers in slightly acidic media and the following treatment parallels the one given previously.[7] The positive contribution is produced by the displacement of the hydrogen on the remaining free platinum sites after $Ni(OH)_2$ adsorption:

$$q_H = q_{H,0.1}^{\theta=0}(1 - m\theta_{Ni}) \quad (1)$$

and the negative contribution is attributed to the displacement of OH adsorbed on nickel adatoms

$$q_{OH} = -n\, q_{111}\theta_{Ni} \quad (2)$$

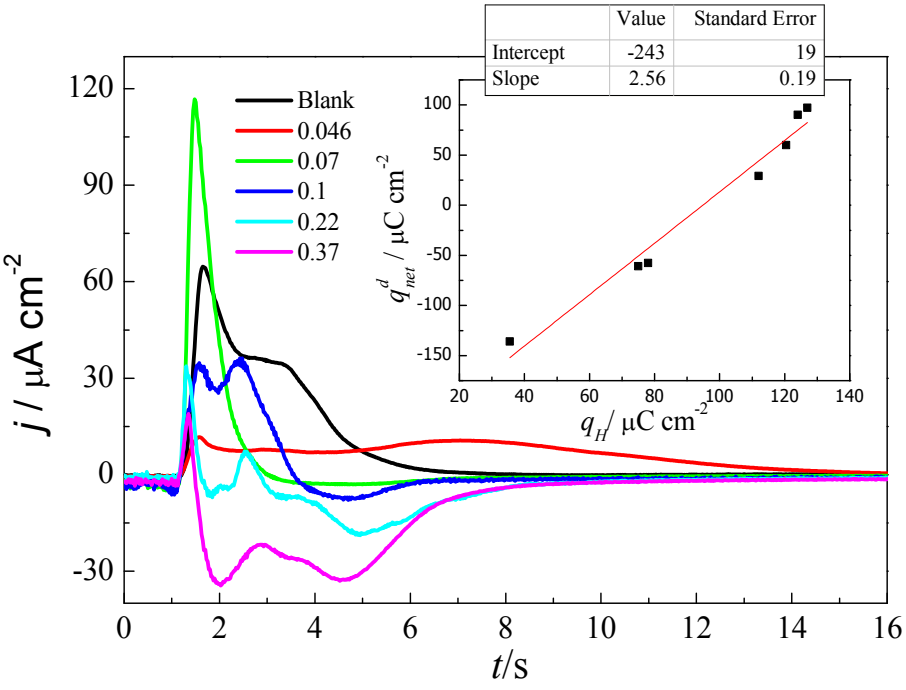


**Figure 4**. CO charge displacement curves for different Ni coverages ($\theta_{Ni}$). The transient current is registered versus time at 0.1 V during CO adsorption. When Ni coverage increases, the positive current decreases, while a negative current appears. The insert shows the plot of the net displaced charge versus the voltammetric hydrogen charge for each nickel coverage. Comparing the equation obtained from the plot with equation 5, it is possible to determine the ratio of n/m.

where $q_{H,0.1}^{\theta=0}$ is the hydrogen charge on the blank experiment recorded at 0.1 V in the absence of nickel (126 μC/cm$^2$), $q_{111}$ is the charge corresponding to one electron per Pt atom on the (111) surface (240 μC/cm$^2$), n is the stoichiometry OH/Ni and m is the number of Pt atoms blocked by each nickel adatom. Therefore, the displaced net charge ($q_{net}^{d}$) is the addition of the positive and negative contributions.[7]

$$q_{net}^{d} = q_{H,0.1}^{\theta=0}(1 - m\theta_{Ni}) + (-n\, q_{111}\theta_{Ni}) \quad (3).$$

A second piece of information is given by the voltammetric charge, which is attributed only to hydrogen adsorbed on Pt since OH coverage is not expected to change during potential cycling in the low potential region (this is different in acid solution).[7] The voltammetric charge related with hydrogen UPD at the different nickel coverage ($q_H$), can be expressed by the equation:

$$q_H = q_H^{total}(1 - m\theta_{Ni}) \quad (4)$$

where $q_H^{total}$ is the hydrogen charge on the blank experiment in the absence of nickel (140 μC/cm$^2$) and m is the number of Pt atoms blocked by each nickel adatom. This equation relates hydrogen UPD charge with $Ni(OH)_2$ coverage.

Combining the equations (3) and (4) we can obtain a relationship between the displaced net charge and the hydrogen charge from the voltammetric profiles for each nickel coverage.

$$q_{net}^{d} = \left(\frac{n}{m}q_{111} + q_{H,0.1}^{\theta=0}\right)\frac{1}{q_H^{total}}q_H + \left(-q_{111}\frac{n}{m}\right) \quad (5).$$

The plot of the net displaced charge versus the voltammetric hydrogen charge, $q_H$, for each nickel coverage (insert figure 4) is linear as suggested by equation (5). From the slope (2.56 ± 0.19) and the intercept (243 ± 19 μC cm$^{-2}$), it is possible to obtain the relationship between m and n. A ratio of (n/m) nearly equal to 1 is obtained. This means that the OH/Ni stoichiometry is equal to the Pt/Ni stoichiometry. Therefore, if we assume that the nickel species adsorbed on the surface is $Ni(OH)_2$, this would indicate that two platinum atoms on the surface are occupied by one nickel atom (m=2). Knowing the Pt/Ni stoichiometry, we can easily obtain the nickel coverage ($\theta_{Ni}$) from equation (1). These results fit relatively well if we assume that $Ni(OH)_2$ arrange on Pt(111) surface forming a monolayer, which is a reasonable assumption considering the low Ni(II) amount. However, it is important to remark that some authors have reported that $Ni(OH)_2$ tends to

rearrange forming 3D clusters following a Volmer-Weber (VW)-type growth with a height equivalent to two layers.[4] Still, the proposal of 2D growth at low coverage provides a coherent balance between the charge associated with hydrogen UPD and $OH^-$ adsorption, according to the CO displacement measurements. Alternatively, it would be possible that, even if clusters are composed of more than one nickel layer, CO only displaces OH bonded to the top layer or even that OH only adsorb on the upper nickel layer. In this case, the coverage calculated would have the meaning of a projected coverage on the platinum surface.

The voltammetric charges in the OH adsorption region, above 0.3 V (figure 1A) can also be analyzed following similar coulometric equations. In this way, the correlation between OH and hydrogen charges can be investigated. The charge involved in nickel oxidation would be:

$$q_{OH}^{Ni} = q_{111}\theta_{Ni}\beta \quad (6)$$

where β is the number of electrons for each $Ni(OH)_2$. This would be 1 if we assume that nickel oxidation to +3 state takes place in this potential region, $Ni(OH)_2 + OH^- \rightarrow NiOOH + H_2O + e$.

The OH charge can be described by the following equation:

$$q_{OH}^{\mathrm{Pt}} = q_{OH}^{Blank}(1 - m\theta_{Ni}) \quad (7)$$

Combining the equations (1), (6) and (7), we can obtain the relation between the charge of nickel and OH versus the hydrogen charge:

$$q_{OH}^{Ni} + q_{OH}^{Pt} = \left(\frac{q_{OH}^{Blank}}{q_H^{total}} - \frac{q_{111}\beta}{q_H^{total}m}\right)q_H + \frac{q_{111}\beta}{m} \quad (8)$$

Here, $q_{OH}^{Ni} + q_{OH}^{Pt}$

represents the total charge integrated between 0.4 and 0.9 V. By plotting the latter as a function of the hydrogen charge, a straight line is expected according to equation (8), from which the ratio between m and β can be obtained from the slope or from the intercept. The result is shown in figure 5, from which a ratio of β/m ≈1 is obtained. This result implies that if m = 2, the β value is 2, indicating that there is one extra electron in the electronic balance of the nickel oxidation reaction. This result is unexpected from the known stoichiometric reactions of Ni, because it suggests an extra OH adsorbing on the

surface. Therefore, it may also indicate the formation of two nickel layers in which case there are two OH adsorbing by each Pt blocked.

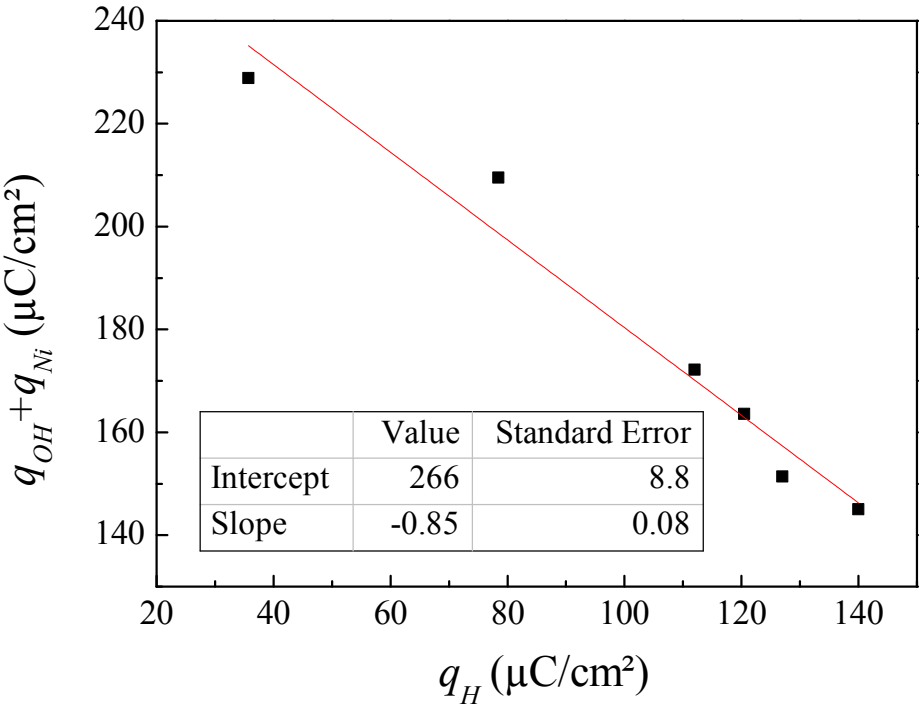


**Figure 5**. Relationship between charge of nickel and OH versus the hydrogen charge.

Next, we show the analysis of the CO oxidation charges obtained after the charge displacement experiments. Figure 6 shows the integrated charges under the CO stripping peaks, plotted as a function of nickel coverage. In addition of the total charge integrated between 0.2 and 0.9 V, partial charges for the peak at ca. 0.5 V (P1) and the peak at ca. 0.75 V (P2) are also shown. All of the plotted charges have been corrected to account for the charge involved in the OH adlayer recovery that must take place after the CO oxidation. From 0.06 to 0.66 (P1), the correction should account for the recovery of the displaced OH ions that have taken place during the charge displacement, while from 0.66 to 0.88 (P2), it should consider the nickel oxidation. In both cases (for P1 and total

charge), the correction can be obtained from the combination of the displacement and voltammetric charges according to the equation:

$$q_{CO} = q_{stripping} - q(0.1 - E) + q_{net}^{d} \quad (9)$$

where $q(0.1 - E)$ is the integrated charge from the voltammograms without CO (figure 1A) between 0.1 V and the potential limit, *E*, used to obtain the CO charge (0.66 and 0.88 for P1 and total charge, respectively). For the integration of P2, green symbols in figure 6, the difference between $q(0.1 - 0.66)$ and $q(0.1 - 0.88)$, which is the same as $q(0.66 - 0.88)$, is used as correction.

As can be seen in figure 6, when nickel coverage increases, P1 increases while P2 decreases. Therefore, it is reasonable to attribute P1 to the oxidation of CO on nickel while P2 would be the oxidation of CO on platinum. For the maximum nickel coverage attained, P2 drops to nearly zero indicating that most of the surface is covered by nickel. Concurrently to this, there is a rise in the CO oxidation charge between 0.06 and 0.66. This reflects a catalytic effect favored by the increment of nickel hydroxide. On the other hand, the total CO charge (black symbols) remains nearly constant, except for the highest nickel coverage where a decrease of both P1 and total charge is observed. This could reflect a change in the electronic properties of the nickel clusters at the highest coverage, that can accommodate a lower amount of CO or it could be due to a stronger adsorption of OH on nickel that would be more difficult to be displaced by CO, resulting in a lower coverage of the latter.

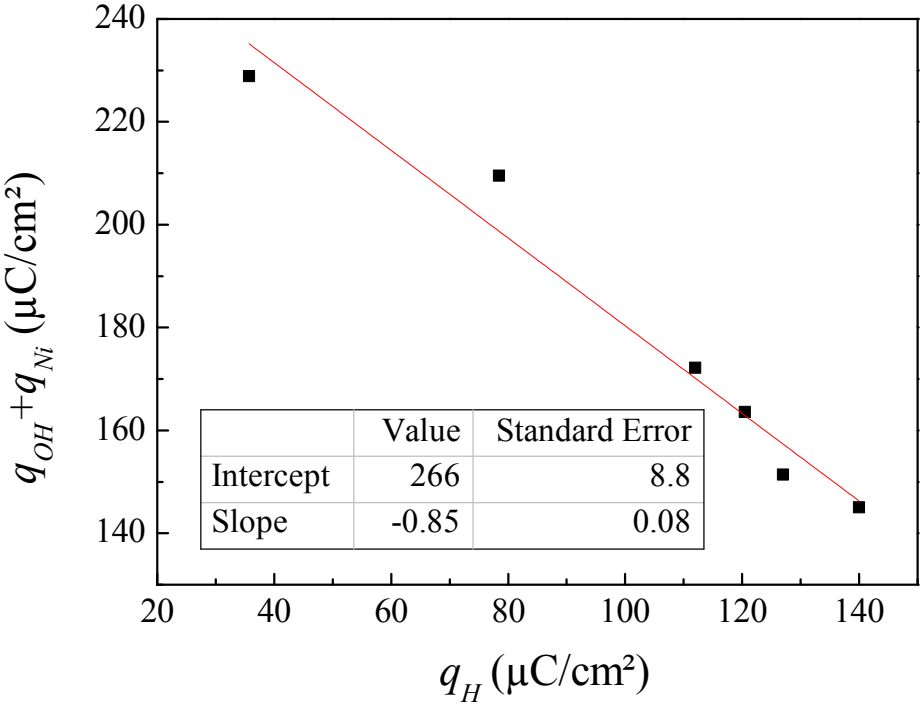


**Figure 6**. Plot of the CO charge obtained from stripping after the CO displacement experiments, versus nickel coverage. Black squares: total charge (from 0.06 to 0.88), Red circles: integrated charge from 0.06 to 0.66 V (peak 1), Green triangles: integrated charge from 0.66 to 0.88 (peak 2).

As discussed in previous work,[16] the total charge can be obtained from the integration of voltammetric curves using the CO displaced charge at 0.1V as the integration constant. Fig 7A and 7B show the total charge/potential curves obtained for different nickel coverages, according to the following equation:[16]

$$q(E) = q(E^*) + \int_{E^*}^{E} \frac{j}{v} dE \quad (10)$$

where $j$ is the voltammetric current, $v$ is the sweep rate, $E^*$ is the potential of the CO charge displacement experiment and $q(E^*)$ is the corresponding total charge at this potential. To obtain the latter, displaced charges need to be corrected to consider the remaining charge on the CO covered surface:

$$q_d^{Net} = q_{CO} - q(E^*) \quad (11)$$

where $q_{CO}$ is the interfacial charge on the CO covered electrode that can be calculated according to equation (12).

$$q_{CO} = \int_{Epzc}^{E^*} C_{CO} dE \quad (12)$$

where the pzc of the CO covered surface is around 1.0 V (SHE)[17, 18] and $C_{CO}$ is the differential capacity of the CO covered interphase (25 μF/cm$^2$ for pH 13 in Pt(111)) that has been obtained from the voltammetric current in a narrow potential range close to 0.1 V, where any faradaic contribution from CO oxidation is negligible. When nickel coverage increases, the capacitance values are greater, being 34 μF/cm$^2$ for the highest nickel coverage. The contribution to the total displaced charge from $q_{CO}$ in this work, at 0.1 V (RHE) at pH 13 for each nickel coverage, is shown in the supplementary information (Table S1).

Figure 7A shows the voltammetric integrated charge as function of the applied potential using the $q_d^{Net}$ at 0.1V vs RHE as integration constant. Figure 7A clearly shows that the pztc, (the potential at which the q vs E curve cross the x-axis) is significantly shifted to lower potentials by increasing the $Ni(OH)_2$. This is a consequence of the increase of adsorbed OH, which contributes as positive total charge on the metal. Calculated values of pztc for all $Ni(OH)_2$ coverages are tabulated in Table 1. Remarkably, for the higher values of $\theta_{Ni}$, negative pztc values were calculated, well below the HER onset.

It should be stressed at this point that total charge plotted here includes also charge involved in adsorption processes and therefore differs from the free charge. Therefore, the shift to lower potentials of the pztc does not imply that the charge and, consequently, the electric field at the interphase, are more positive at the onset of HER. An alternative description of the interphase would consist on counting only the charge on platinum while considering the OH on nickel as part of the metal: This description would stress the electronic effect of nickel on platinum electrode and would give a better idea of the changes induced by Ni on the free charge. With this idea, we have displayed in figure 7B corrected *q vs E* curves after the subtraction of the charge corresponding to OH from $Ni(OH)_2$. The pztc (Table 1, pztc $_{OH\ corr}$) obtained from the curves shown in fig 7B provides values that are approaching the onset of HER but are always above it.

| $\theta_{Ni}$ | pztc | pztc $_{OHcorr.}$ |
|---|---|---|
| **0** | 0.675 | 0.675 |
| **0.046** | 0.653 | 0.692 |
| **0.07** | 0.361 | 0.674 |
| **0.1** | 0.256 | 0.58 |
| **0.22** | -0.123 | 0.088 |
| **0.37** | -0.503 | 0.048 |

**Table 1**. pztc for each nickel coverages with and without OH correction. The pztc values corresponding to the higher nickel hydroxide coverages without OH correction were obtained by linear extrapolation, and therefore are subject to a large error. They are included only to illustrate the large expected shift of the pztc.

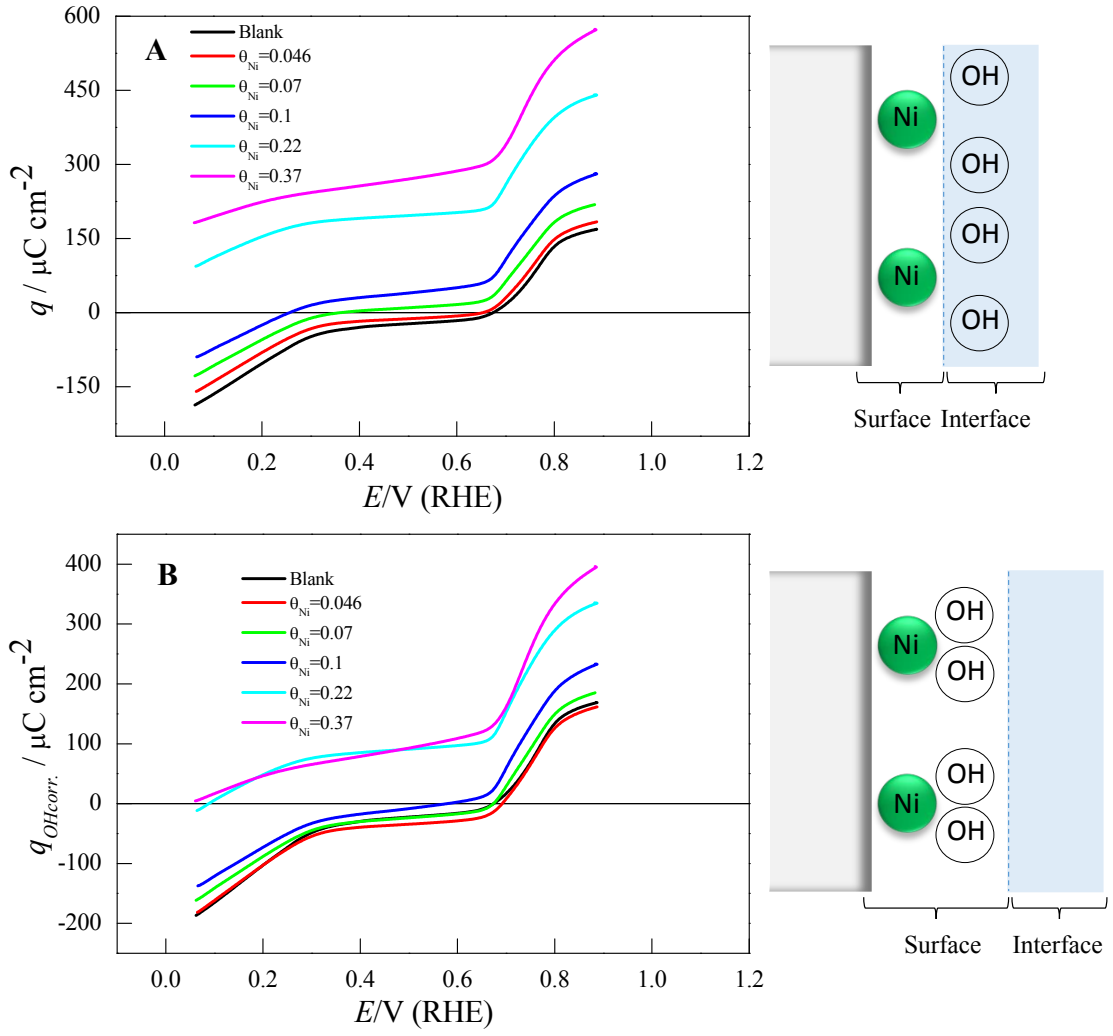


**Figure 7**. *q* vs *E* curves A) without the OH correction (on the right it is shown a schematic representation of the surface electrode considering the OH as part of the interface) and

B) with the OH correction (in this case the OH is considered as part of the material). In both cases, charges are corrected to account for the residual charge after CO adsorption.

### *3.4) Laser temperature jump technique*

Results of the CO displacement technique reveal that the increase of the $Ni(OH)_2$ coverage on Pt(111) shifts the pztc to more negative potentials. This technique gives a measure of the total charge on the metal surface, which contains both faradaic and capacitive (free charge) contributions, the former being considerable larger (in absolute value). Even after the correction to subtract OH contribution shown in figure 7B, the measured charge still contains the hydrogen contribution. From CO displacement transients, information about the nature of adsorbed species can be inferred, allowing the distinction between adsorbed hydrogen or hydroxide. However, it does not allow a direct measure of the free charge separation at the interphase, which is at the origin of the electric field on the surface. If the shift of the pztc is paralleled by a similar negative shift in the pzfc, results obtained in the sections above would suggest that the presence of $Ni(OH)_2$ clusters on Pt(111) increases the electric field at the surface for E>pzfc (i.e. the surface holds a higher positive charge) while the electric field would decrease or would be even inverted for E<pzfc. This fact could promote the hydroxide adsorption at lower applied potentials in comparison to Pt(111) as well as the stronger OH chemisorption on Ni. However, these trends need to be verified before concluding how the presence of $Ni(OH)_2$ clusters affects the capacitive charge on the metal side.

In this regards, additional information can be obtained from the laser temperature jump technique that provides information intimately linked to the magnitude and sign of the electric field at the interphase. In this technique, the temperature of the interphase is suddenly changed using pulsed laser irradiation and the coulostatic change of the electrode potential is monitored as response to the change of temperature. This potential variation mainly responds to changes in the restructuration of the double layer as a result of the temperature increase. Details of the technique have been given previously.[9, 10, 19] These previous works demonstrated that the change of the electrode potential with the temperature is mainly due to a decrease of the dipolar contribution caused by the sudden temperature increase. Therefore, the sign and magnitude of the potential transient is related with the orientation of solvent molecules at the interphase. At potentials lower than the pzfc, where the surface is negatively charged, the dipolar contribution is positive

(water molecules orientate with the hydrogens pointing out the surface) and negative transient *ΔE vs t* are recorded. On the opposite side, applied potentials higher than pzfc (water molecules orientated with the oxygen towards the surface) leads to positive laser induced potential transients. In between there would be a potential where transients are nearly zero, implying that there is no net dipolar contribution, i.e., there is maximum disorder in the water network. Such corresponds to the potential of maximum entropy of double layer formation, pme, a value that is close to the pzfc.[20, 21]

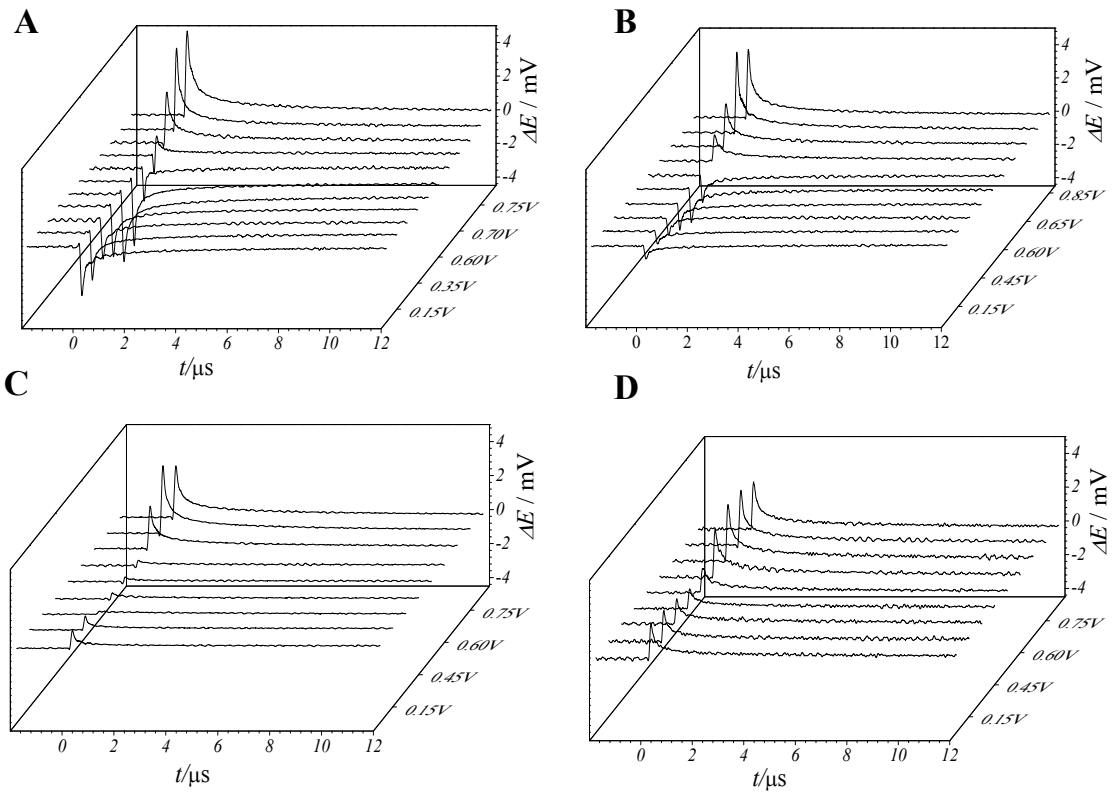


**Figure 8**. Laser ΔE vs t transients recorded on Pt(111) modified with different coverages of $Ni(OH)_2$. A) Bare Pt(111) B)$\theta_{Ni}$= 0.1 C)$\theta_{Ni}$=0.2 and D)$\theta_{Ni}$= 0.37 Laser beam energy: 0.8 mJ.

Figure 8 shows laser *ΔE-t* transients recorded in a wide potential region (from 0.10V to 0.85V) and for different $Ni(OH)_2$ coverages (θ) ranging between 0 and 0.37. It is worth noting that most of these transients show a monotonic decay, following the expected relaxation profile of the temperature. On the other hand, non-monotonic decays have been reported previously, especially in the hydrogen adsorption region, when charge transfer reactions associated with adsorption processes take place.[21] Therefore, we can conclude

that, in the present case, faradaic reactions in the hydrogen region are too slow and therefore decoupled from the double layer response in the microsecond time scale. This agrees with the reported decrease in the hydrogen adsorption rate measured with impedance spectroscopy[6] in alkali vs acid solutions. On the other hand, the analysis of the transients in the region of OH adsorption is more complex. We give below a brief discussion and the complete analysis will be the subject of a future report.

Figure 8A contains the laser transients for the Pt(111)|0.1MNaOH interface. At lower applied potentials, laser transients are negative suggesting that the electric field at the interphase points towards the surface in the hydrogen UPD region. By increasing the applied potential, the magnitude of the transients decreases. At around 680 mV vs RHE the transients change sign and become positive, suggesting that the electric field above this threshold becomes positive (pointing towards the solution). The change of the sign in the recorded transients appears to be located at the onset of the hydroxide adsorption, a result that would indicate that the pzfc is also positioned close to this region.

However, these results do not agree with the trend observed for the shift of the pme in acid and neutral solutions[21, 22] and also disagree with the estimation extrapolated from CO displacement experiments which positioned the pzfc at more positive potentials in the Pt oxide region in alkaline media.[16] According to the results of the laser induced T-jump experiment in acid and neutral media, the pme of Pt(111) does not depend on pH (300mV vs SHE). If this invariability is maintained in alkaline solution, an extrapolated value located around 1.08V vs RHE in 0.1M NaOH would be obtained.[21, 22] These results are supported by the CO displacement technique that also showed a constant value for the pzfc extrapolated from the double layer region that would lie in the Pt oxide region in alkaline media.[16] Contrarily to these results, the laser technique shows the transient changing sign at around -680mV. All these observations deserves considering different scenarios to the location of the pme for Pt(111) in alkaline solution. One possibility would be that the extrapolated values are not valid simply because they would correspond to a hypothetical pzfc for an OH free surface. However, the adsorption of OH may most likely exert electronic changes shifting the pzfc to the value measured with the laser experiment.[23, 24] Another possibility is that the assumption made about the decoupling of faradaic and capacitive responses attained in the time scale of the laser experiment fails in this case. At this point, it must be mentioned that in the present case a bipolar transient was obtained at 680mV vs RHE (Figure 8A) rather than the predicted zero value transient,

although for E>700mV laser transients are already monotonic and positive. Then, another possibility is that the change of the sign in the laser transients close to the onset of hydroxide adsorption is actually related with the kinetics of hydroxide adsorption rather than reflecting a reorientation of the water molecules[6]. This would agree with impedance spectroscopy measurement that failed to decouple faradaic and capacitive responses for measurements up to 1 MHz[25] therefore implying that rate of OH adsorption is extremely fast.[26]

Although the uncertainty just discussed above does not allow to give an unambiguous location for the pme of Pt(111) in alkaline solutions, interesting conclusions can still be drawn from the sign and magnitude of the transients at lower potentials and their variation with nickel coverage. Introducing $Ni(OH)_2$ with a coverage up to 0.1 (Figure 8B) causes that the laser transients recorded in the lowest potential region decrease in intensity, but they are still negative, i.e, the average water molecule orientation is with the hydrogens pointing towards the surface. These results evidence that the presence on $Ni(OH)_2$ decreases the ordering in the interfacial network of water molecules. In the potential region dominated by hydroxide adsorption (potentials higher than 700mV vs RHE), laser transients are positive and show similar magnitude to those previously recorded on bare Pt(111). Further increasing the $Ni(OH)_2$ coverage (Figure 8C and 8D) causes that the laser transients in the lowest potential region approach to zero at $\theta_{Ni(OH)_2} = 0.2$ and they become positive at $\theta_{Ni(OH)_2} = 0.37$, the latter coverage only achievable by using the flow cell. These results show that partially covering the Pt(111) surface with $Ni(OH)_2$ modifies the distribution of capacitive charges increasing the electric field (increasing charge separation) in the potential region close to the onset of anion adsorption while decreasing it at the onset of HER.

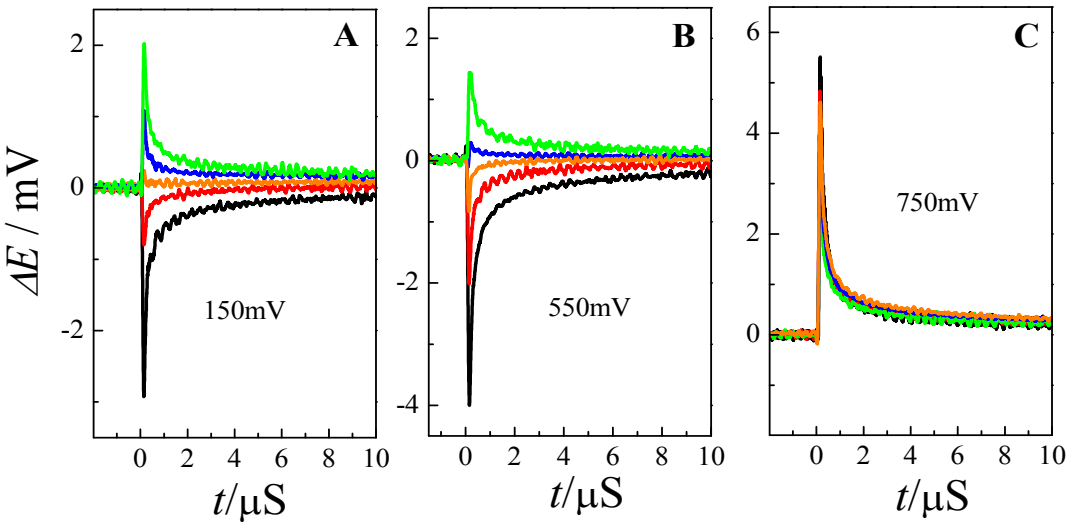


**Figure 9**. Laser transients for different $Ni(OH)_2$-Pt(111) coverages at- A) 150mV, B) 550mV, C) 750mV. Color legend: Black) Pt(111), and $\theta_{Ni}$= red) 0.1, orange) 0.15, blue) 0.22 , green) 0.37.

Figure 9A, 9B and 9C compare the transients recorded for different $Ni(OH)_2$ coverages and three different applied potentials: 150mV, 550mV and 750mV vs RHE. The comparison between laser transients for different $Ni(OH)_2$ coverages clearly evidences that the increase of $Ni(OH)_2$ on the surface decreases the negative electric field in both the double layer and the hydrogen UPD region. On the other hand, the laser transients recorded at 750mV with the different surface coverages almost overlap, suggesting that the adsorbed $OH^-$ may shield the charge on the substrate, independently of the $Ni(OH)_2$ coverage.

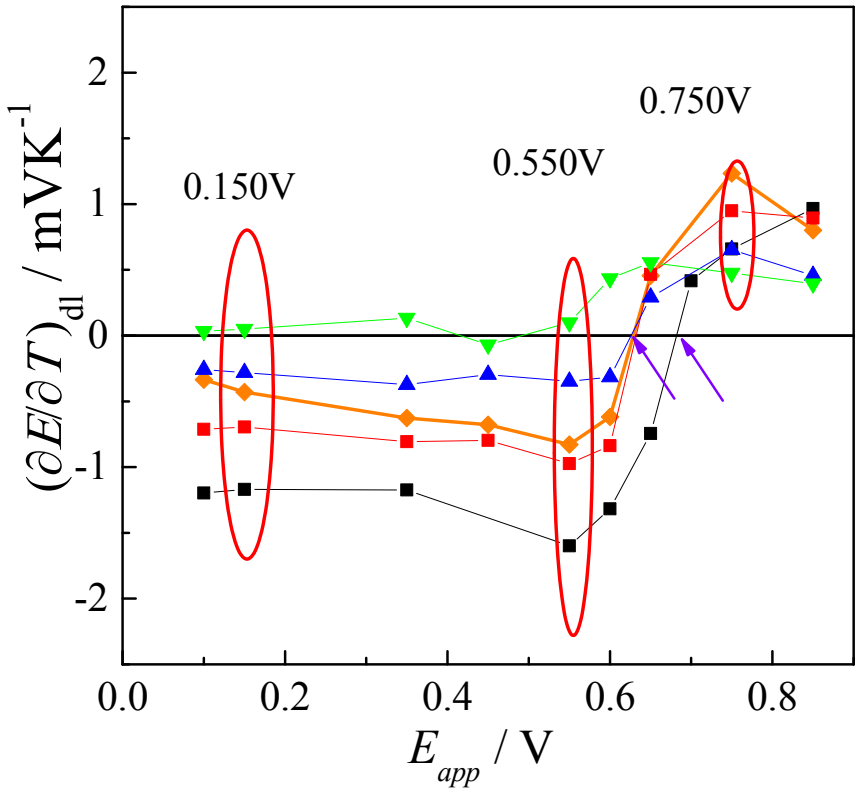


**Figure 10**. Thermal coefficients for Pt(111) electrode with different coverages of Ni(OH)2. Color legend: Black) Pt(111), and $\theta_{Ni}$= red) 0.1, orange) 0.15, blue) 0.22, green) 0.37.

It has been previously demonstrated that a more quantitative analysis of the laser induced potential transients can be achieved by analyzing the temperature evolution during heat dissipation, after laser irradiation, which follows a $1/t^{1/2}$ dependence, being the potential change with the temperature:

$$\Delta E = \frac{1}{2}\frac{\partial E}{\partial T}\Delta T_0\sqrt{\frac{t_0}{t}} \quad (13)$$

In this way, linearization of the laser transients allows calculating the thermal coefficients of the double layer formation ($\frac{\partial E^M}{\partial T}$), i.e. by plotting $\Delta E$ *vs* $t^{-1/2}$ (see Figure S3). Figure 10 plots the ($\frac{\partial E^M}{\partial T}$) coefficients obtained at different applied potentials ranging from 100mV to 850mV. It shows that the ($\frac{\partial E^M}{\partial T}$) values increase between 100 mV and 700mV as $\theta_{Ni(OH)2}$

increases, and they become positive in the whole potential region of interest for the highest $\theta_{Ni(OH)2.}$ In this case, the thermal coefficients were corrected to account for the thermodiffusion effect, i.e., the contact potentials that appears due to the temperature difference between the solutions surrounding the reference and working electrodes. This can be calculated from the Eastman entropies of transport and mobilities of the ions[27], amounting to 0.43 $mVK^{-1}$ in 0.1M NaOH.[28] Contribution of the thermodiffusion potential is usually negligible, but not in this case due to the abnormally high mobility of $OH^-$ anions (see the supporting information for more information about the correction of the thermodiffusion effect). The thermal coefficients without thermodiffusion correction are shown in figure S5 for comparison while figure S4 shows the error in the estimation of the thermal coefficients. As can be seen in figure 10, after the correction, only at the highest coverage, $\theta_{Ni(OH)2} = 0.4$, the thermal coefficients approach zero or are slightly positive in the hydrogen UPD region. It must be highlighted that the potential at which $\left(\frac{\partial E^M}{\partial T}\right)=0$ on bare Pt(111) shifts more than 50mV to lower values by increasing the $\theta_{Ni(OH)2}$ (marked with arrows in Figure 10) results that are in agreement with those obtained from CO-displacement measurements. All these results confirm that the presence of $Ni(OH)_2$ on Pt(111) shifts the pzfc of Pt(111)|0.1M NaOH to values that would be closer to the onset of the hydrogen evolution reaction, especially for those at sufficiently high $\theta_{Ni(OH)2.}$ More importantly, the decrease in magnitude of the potential transients evidences a significant decrease in the ordering of the network of water molecules in the vicinity of the electrode.

### *3.5) Discussion of the results*

Results from the laser induced temperature jump technique are consistent with those from CO displacement when the $OH^-$ displacement charge is considered. Both experiments consistently show that the modification of Pt(111) with $Ni(OH)_2$ highly influences the charge distribution in the Pt(111)|alkaline solution interfacial region and shifts the pztc/pzfc values closer to the HER onset. Increasing the $Ni(OH)_2$ coverage decreases the magnitude of the negative electric field in the lower voltammetric potential region, a fact that implies a higher disorder in the solvent dipole network than in the absence of $Ni(OH)_2$. The rate of the HER is kinetically enhanced and the required overpotential lowered by the presence of $Ni(OH)_2$. In particular, the improvement of the HER for the highest $Ni(OH)_2$ coverage is remarkable. These experimental observations strongly support the idea that the enhancement of HER on Pt(111) with $Ni(OH)_2$ may be related

to the interfacial charge and solvent redistribution. $Ni(OH)_2$ retains partial charge on Pt(111) and disrupts the water molecular network, a fact that seems to enhance the charge transfer for the HER. Foregoing results reinforce the experimental evidence reported recently by Ledezma et. al.,[6] and the model for HER in which the interfacial water network becomes easier to reorganize due to the lowering of the interfacial electric field caused by the presence of a small amount of $Ni(OH)_2$. Figure 11 shows a scheme of how $Ni(OH)_2$ affects the water dipole structuration and charge distribution.

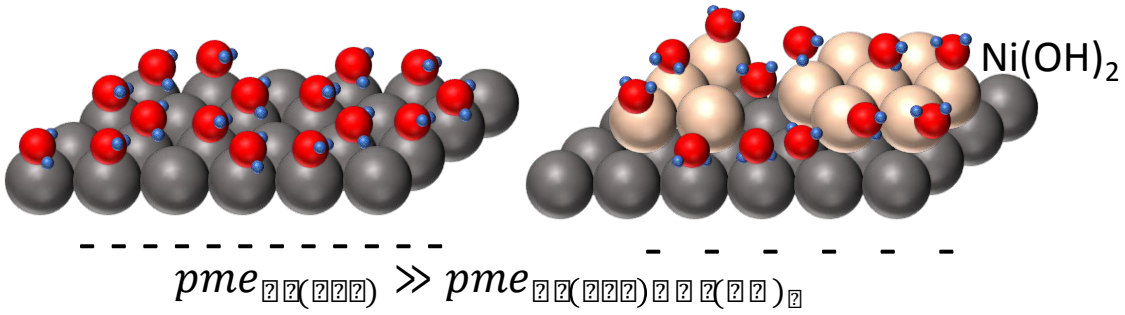


**Figure 11**. Schematic representation of the network of water dipoles on Pt(111) and the unstructured network on the $Ni(OH)_2$ modified surface, due to a change in the interfacial electric field. For Pt(111) the water dipole network is ordered, but the nickel presence induces a disorder in the water structure which is greater when the nickel coverage increases.

For the highest nickel coverage a major HER efficiency is observed. For this coverage, laser experiments reveal that the electric field is even slightly positive in the hydrogen UPD region. This conclusion is supported by CO displacement experiments that showed the presence of adsorbed hydroxide species, overlapped with the hydrogen UPD. CO displacement and laser temperature jump suggest that $Ni(OH)_2$ shifts the Pt(111)|0.1M NaOH potential of zero transient to values closer to the onset potential of HER, facilitating the O-H scission step by diminishing the energetic barrier for charge movement through the structured water network.

## 4) Conclusion

In this work, different $Ni(OH)_2$ coverages on Pt(111) electrodes have been prepared and their effect on the hydrogen evolution reaction (HER) was investigated. To this end, we combined CO displacement experiments with laser-induced temperature-jump techniques to probe how the presence of $Ni(OH)_2$ influences the interfacial charge and the distribution of solvent dipoles in the interfacial region. Coulometric analysis helped us to establish stoichiometric relationships between OH, Ni and Pt. Results obtained with CO displacement technique reveal that the pztc shifts to lower potentials by progressively increasing the $Ni(OH)_2$ coverage, i.e., the net total charge (including adsorption processes) in the hydrogen UPD region becomes less negative. This result would support that the presence of $Ni(OH)_2$ shifts the onset of anion/hydroxide adsorption to potentials values lower than those for bare Pt(111), which is also consistent with the enhancement of the CO oxidation rate under the presence of $Ni(OH)_2$.

To obtain more insight about the distribution of free interfacial charge at $Ni(OH)_2$ modified Pt(111) surface, we used the laser-induced temperature-jump technique. The experimental results have revealed a progressive inversion in the signal and a decrease in the thermal coefficient with increasing nickel coverage in alkaline media. This implies a decrease of the electric field caused by a negative shift of the pzfc, an effect more pronounced with a higher amount of $Ni(OH)_2$ on the Pt(111) surface. This lowering of the negative electric field leads to a more facile reorganization of the interfacial solvent molecules facilitating charge transfer through the double layer, thus enhancing HER efficiency.

## Acknowledgements

The authors thankfully acknowledge financial support from the MICINN (Spain) through project CTQ2016-76221-P. P. Sebastian acknowledges to MECD the award of a FPU grant. F. Sarabia acknowledges to Ministerio de Economia, Industria y Competitividad (PEJ-2014-A-57942/PEJ-2014-P-00295).

**Supporting information**: Potential dependence for the band frequency of CO adsorbed on nickel and platinum. Contribution to the total displaced charge from the residual charge on the CO covered surface. Details for the calculation of thermal coefficient of the double layer from laser induced temperature jump experiments. Values of uncorrected thermal coefficients without subtracting the thermodiffusion contribution.

## References

(1) Bockris, J. O. M. The Origin of Ideas on a Hydrogen Economy and Its Solution to the Decay of the Environment. *Int. J. Hydrogen Energ.* 2002, 27, 731-740.

(2) Subbaraman, R.; Tripkovic, D.; Chang, K. C.; Strmcnik, D.; Paulikas, A. P.; Hirunsit, P.; Chan, M.; Greeley, J.; Stamenkovic, V.; Markovic, N. M. Trends in Activity for the Water Electrolyser Reactions on 3d M(Ni,Co,Fe,Mn) Hydr(Oxy)Oxide Catalysts. *Nat. Mater.* 2012, 11, 550-557.

(3) Bockris, J. O. M.; Reddy, A. K. N. *Modern Electrochemistry*. Plenum: New York, 1970.

(4) Subbaraman, R.; Dusan, T.; Strmcnik, D.; Chuang, K.-C.; Masanobu, U.; Paulikas, A. P.; Stamenkovic, V.; Markovic, N. M. Enhancing Hydrogen Evolution Activity in Water Splitting by Tailoring $Li^+$-$Ni(OH)_2$-Pt Interfaces. *Science* 2011, 334, 1256-1260.

(5) Zeng, Z.; Chang, K.-C.; Kubal, J.; Markovic, N. M.; Greeley, J. Stabilization of Ultrathin (Hydroxy)Oxide Films on Transition Metal Substrates for Electrochemical Energy Conversion. *Nature Energy* 2017, 2, 17070.

(6) Ledezma-Yanez, I.; Wallace, W. D. Z.; Sebastián-Pascual, P.; Climent, V.; Feliu, J. M.; Koper, M. T. M. Interfacial Water Reorganization as a Ph-Dependent Descriptor of the Hydrogen Evolution Rate on Platinum Electrodes. *Nature Energy* 2017, 2, 17031-17037.

(7) Sarabia, F. J.; Climent, V.; Feliu, J. M. Underpotential Deposition of Nickel on Platinum Single Crystal Electrodes. *J. Electroanal. Chem.* 2017, 819, 391-400.

(8) Climent, V.; Gómez, R.; Feliu, J. M. Effect of Increasing Amount of Steps on the Potential of Zero Total Charge of Pt(111) Electrodes. *Electrochim. Acta* 1999, 45, 629-637.

(9) Climent, V.; Coles, B. A.; Compton, R. G. Coulostatic Potential Transients Induced by Laser Heating of a Pt(111) Single-Crystal Electrode in Aqueous Acid Solutions. Rate of Hydrogen Asorption and Potential of Maximum Entropy. *J. Phys. Chem. B* 2002, 106, 5988-5996.

(10) Climent, V.; Coles, B. A.; Compton, R. G. Laser-Induced Potential Transients on a Au(111) Single-Crystal Electrode. Determination of the Potential of Maximum Entropy of Double Layer Formation. *J. Phys. Chem. B* 2002, 106, 5258-5265.

(11) Herrero, E.; Li, J.; Abruna, H. D. Electrochemical, in-Situ Surface Exafs and Ctr Studies of Co Monolayers Irreversibly Adsorbed onto Pt(111). *Electrochim. Acta* 1999, 44, 2385-2396.

(12) Garcia, G.; Rodriguez, P.; Rosca, V.; Koper, M. T. M. Fourier Transform Infrared Spectroscopy Study of CO Electro-Oxidation on Pt(111) in Alkaline Media. *Langmuir* 2009, 25, 13661-13666.

(13) Zhao, M.; Wang, K.; Scherson, D. A. In Situ Potential Difference Fourier Transform Infrared Reflection Absorption Spectroscopic Studies of the Electrochemical Oxidation of Adsorbed Carbon Monoxide on Nickel in Alkaline Solutions. *J. Phys. Chem.* 1993, 97, 4488.

(14) Bailey, R. B.; Iri, T.; Richards, P. L. Infrared Spectra of Carbon Monoxide on Evaporated Nickel Films: A Low Temperature Thermal Detection Technique. *Surf. Sci.* 1980, 100, 626-646.

(15) Primet, M.; Dalmon, J. A.; Martin, G. A. Adsorption of Co on Well-Defined Ni/$Sio_2$ Catalysts in the 195–373 K Range Studied by Infrared Spectroscopy and Magnetic Methods. *J. Catal.* 1977, 46, 25-36.

(16) Rizo, R.; Sitta, E.; Herrero, E.; Climent, V.; Feliu, J. M. Towards the Understanding of the Interfacial Ph Scale at Pt(111) Electrodes. *Electrochim. Acta* 2015, 162, 138-145.

(17) Weaver, M. J.; Chang, S. C.; Leung, L. W. H.; Jiang, X.; Rubel, M.; Szklarczyk, M.; Zurawski, D.; Wieckowski, A. Evaluation of Absolute Saturation Coverages of Carbon Monoxide on Ordered Low-Index Platinum and Rhodium Electrodes *J. Electroanal. Chem.* 1992, 327, 247-260.

(18) Cuesta, A. Measurement of the Surface Charge Density of Co-Saturated Pt(111) Electrodes as a Function of Potential: The Potential of Zero Charge of Pt(111). *Surf. Sci.* 2004, 572, 11-22.

(19) Climent, V.; Garcia-Araez, N.; Compton, R. G.; Feliu, J. M. Effect of Deposited Bismuth on the Potential of Maximum Entropy of Pt(111) Single-Crystal Electrodes. *J. Phys. Chem. B* 2006, 110, 21092-21100.

(20) Garcia-Araez, N.; Climent, V.; Feliu, J. M. Evidence of Water Reorientation on Model Electrocatalytic Surfaces from Nanosecond-Laser-Pulsed Experiments. *J. Am. Chem. Soc.* 2008, 130, 3824-3833.

(21) Garcia-Araez, N.; Climent, V.; Feliu, J. Potential-Dependent Water Orientation on Pt(111), Pt(100), and Pt(110), as Inferred from Laser-Pulsed Experiments. Electrostatic and Chemical Effects. *J. Phys. Chem. C* 2009, 113, 9290-9304.

(22) Sebastian, P.; Martinez-Hincapie, R.; Climent, V.; Feliu, J. M. Study of the Pt (111) | Electrolyte Interface in the Region Close to Neutral Ph Solutions by the Laser Induced Temperature Jump Technique. *Electrochim. Acta* 2017, 228, 667-676.

(23) Huang, J.; Malek, A.; Zhang, J.; Eikerling, M. H. Non-Monotonic Surface Charging Behavior of Platinum: A Paradigm Change. *J. Phys. Chem. C* 2016, 120, 13587-13595.

(24) Frumkin, A. N.; Petrii, O. A. Potentials of Zero Total Charge and Zero Free Charge of Platinum Group Metals. *Electrochim. Acta* 1975, 20, 347-359.

(25) Sibert, E.; Faure, R.; Durand, R. High Frequency Impedance Measurements on Pt(111) in Sulphuric and Perchloric Acids. *J. Electroanal. Chem.* 2001, 515, 71-81.

(26) Schouten, K. J. P.; van der Niet, M.; Koper, M. T. M. Impedance Spectroscopy of H and OH Adsorption on Stepped Single-Crystal Platinum Electrodes in Alkaline and Acidic Media. *Phys. Chem. Chem. Phys.* 2010, 12, 15217-15224.

(27) Agar, J. N. Thermogalvanic Cells. Wiley-Interscience: New York, 1963; Vol. 3, pp 31-121.

(28) Vayenas, C. G. Interfacial Phenomena in Electrocatalysis. In *Modern Aspects of Electrochemistry*, White, R. E.; Vayenas, C. G.; Gamboa-Aldeco, M. E., Eds. Springer: New York, 2011; Vol. 51.

TOC graphic